

Selective Leaching of LiFePO_4 by H_2SO_4 in the Presence of NaClO_3

HONGHUI TANG^{1,2}, XI DAI^{1*}, QIANG LI², YANCHAO QIAO², FENG TAN²

¹ School of Metallurgy and Environment, Central South University, Changsha, 410083, Hunan, P. R. China

² Hunan Brunp Recycling Technology Co., Ltd, Ningxiang, 410600, Hunan, P. R. China

Abstract: *Herein, problems commonly observed for the wet leaching of waste LiFePO_4 cathode materials, namely extensive Fe leaching and impurity removal, are mitigated through the use of NaClO_3 , and the effects of leaching parameters on Fe, P, Li, and Al leaching efficiencies are probed. As a result, optimal leaching conditions are determined as temperature = 90°C , H_2SO_4 concentration = 1 M, liquid-to-solid ratio = 5:1, leaching time = 1 h, stirring speed = 150 rpm, and NaClO_3 dosage = 25 g per 100 g raw material, with the corresponding Fe, P, Li, and Al leaching efficiencies obtained as 0.21, 0.03, 97.23 and 11.87%, respectively.*

Keywords: *spent lithium iron phosphate, selective leaching, cathode material, battery recycling*

1. Introduction

Methods of spent LiFePO_4 battery disposal include the cascade utilisation and recovery of valuable metals [1,2]. Cascade utilisation aims to ensure the quality and safety of target products but is only applied in some demonstration plants, as the performance of waste batteries is unpredictable [3].

At present, the hydrometallurgical recovery of Li from waste LiFePO_4 batteries is widely employed in the lithium battery recovery industry [4-6]. Zhen et al. [7] leached the LiFePO_4 cathode material with a mixture of H_2SO_4 and H_2O_2 and adjusted the pH of the obtained solution with alkali to precipitate Fe as $\text{Fe}(\text{OH})_3$, further adjusting pH to 5.0–8.0 to remove other heavy metal ions and thus obtain a solution of Li_2SO_4 . The latter solution was treated with solid Na_2CO_3 , concentrated, and crystallised to obtain Li_2CO_3 . The above method consumes large amounts of alkali and produces much slag, therefore not complying with the concept of environmental protection and economy.

Yang et al. [8] probed the effects of mechanochemical activation of spent cathode powder and its potential to achieve selective Li recovery, revealing that after mechanochemical activation, ~97.67% Fe and 94.29% Li could be recovered under optimised conditions. The lixivium was evaporated and concentrated to recover FePO_4 , and the filtrate pH was adjusted to neutral to afford Li_3PO_4 . The above process is lengthy, featuring the drawbacks of high energy/alkali consumption and affording a product with high impurity content. Li et al. [9] found that the use of dilute H_2SO_4 as a leachant and H_2O_2 as an oxidant allows Li to be selectively leached into solution, while Fe and P remain in the residue as FePO_4 , which is different from the traditional process of using excess mineral acid to leach all elements into solution.

Under optimised conditions, Li, Fe, and P leaching efficiencies of 96.85, 0.027, and 1.95%, respectively, were recorded. However, the above study is incomplete, employing an insufficient amount of experimental materials and therefore providing unconvincing results. Moreover, the chemical stability of H_2O_2 is low, the leaching process is prone to overflow, and the achieved oxidation efficiency is far lower than that observed for NaClO_3 and NaClO .

When waste LiFePO_4 cathode material is treated with H_2SO_4 , Fe is solubilised as Fe^{2+} , and its removal consumes large amounts of alkali liquor and produces much solid waste [10,11]. Importantly, the metal value of LiFePO_4 is lower than that of lithium nickel cobalt manganate, which results in low market value and low recovery enthusiasm [12–14]. Herein, LiFePO_4 was leached with H_2SO_4 in the

*email: luckcici1596@163.com

presence of NaClO_3 at controlled $p\text{H}$ and system potential to realise the removal of Fe in the form of insoluble FePO_4 to afford a solution of Li_2SO_4 and thus achieve selective Li leaching.

Thermodynamic analysis of the Li-Fe-P-H₂O system

During the leaching of LiFePO_4 cathode powder by H_2SO_4 , $p\text{H}$ and electric potential control are important for keeping Li in solution and Fe precipitated as FePO_4 [1,12,13], which highlights the need to investigate the ϕ - $p\text{H}$ diagram of the Li-Fe-P-H₂O system (Figure 1). According to the equilibrium reactions in E- $p\text{H}$ Diagrams for the Li-Fe-P-H₂O System from 298 to 473 K [15], ion concentrations of 1 and 0.1 M were used instead of activities.

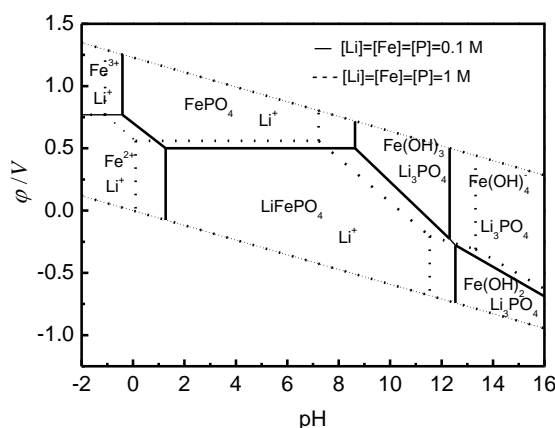
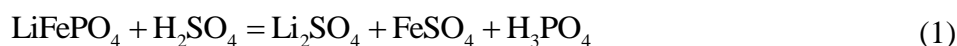


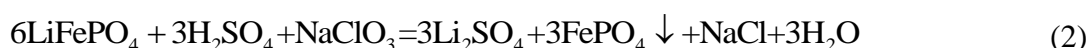
Figure 1. ϕ - $p\text{H}$ diagram of the Li-Fe-P-H₂O system, $T=298.15\text{K}$

Figure 1 shows that the dominant area of FePO_4 in the Li-Fe-P-H₂O system is characterised by high potential and low $p\text{H}$. During the leaching of LiFePO_4 by acid, control of $p\text{H}$ and system potential allows Fe and Li to be present as FePO_4 and Li^+ , respectively, thus enabling selective leaching and FePO_4 isolation.

In the absence of an oxidant, the reaction of LiFePO_4 with H_2SO_4 can be described as



Conversely, a different reaction is observed in the presence of NaClO_3 :



2. Materials and methods

Concentrated H_2SO_4 and NaClO_3 were of analytical-grade purity. Spent LiFePO_4 was provided by Hunan Brunp Recycling Technology Co., Ltd., and contained 4.26 wt% Li, 17.39 wt% P, 32.18 wt% Fe, 2.13 wt% Al, and 44.03 wt% other elements.

A beaker filled with H_2SO_4 of a certain concentration and volume was charged with LiFePO_4 (100 g) and put into a water bath held at a specified temperature and equipped with an overhead mixer. Subsequently, NaClO_3 was added, and after a fixed retention time, the reaction mixture was filtered, and the Fe, P, Li and Al contents of the dry filter cake were determined. The filtration residue was analysed by diffraction of x-rays (XRD Ultima IV, JP) and scanning electron microscope (SEM Apreo C, US). The filtrate was analysed by inductively coupled plasma spectrometry (ICAP 7000SERIES, UK), and leaching efficiency (η_i) was calculated as

$$\eta_i = \frac{m_A - m_a}{m_A} \times 100\% \quad (3)$$

where m_A is the mass of a given element in the raw material, and m_a is the mass of this element in the filter residue.

3. Results and discussions

3.1. Effect of leaching temperature on leaching efficiency

Figure 2 shows the effects of temperature (T) on leaching efficiency at $[\text{H}_2\text{SO}_4] = 1 \text{ M}$, liquid-to-solid ratio (L/S) = 5:1, leaching time (t) = 1 h, NaClO_3 dosage (D) = 25 g, and stirring speed (s) = 150 rpm.

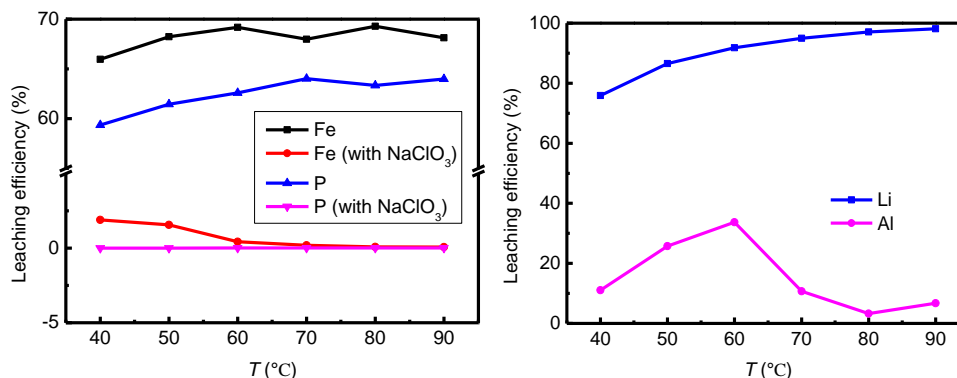


Figure 2. Effect of temperature on leaching efficiency

With increasing T , the leaching efficiency of Li increased, that of Fe declined, and that of P did not significantly change, and that of Al increased first and then decreased. At 90°C , the leaching efficiencies of Fe, P, Li, and Al equalled 0.07, 0.017, 98.12, and 16.72%, respectively. In order to achieve the results of high lithium leaching rate and low iron leaching rate, the above temperature (90°C) was therefore selected as optimal.

3.2. Effect of sulphuric acid concentration on leaching efficiency

Figure 3 shows the effect of $[\text{H}_2\text{SO}_4]$ ($T = 90^\circ\text{C}$, $L/S = 5:1$, $t = 1 \text{ h}$, $D = 25 \text{ g}$, $s = 150 \text{ rpm}$) on the leaching efficiencies of Fe, P, Li, and Al.

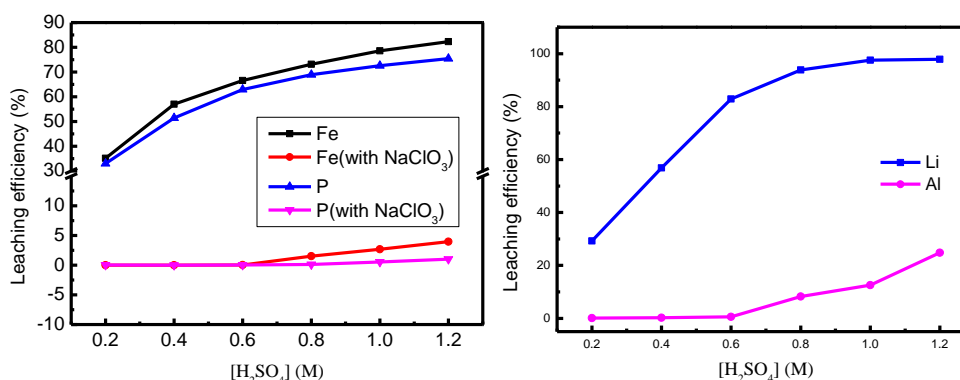


Figure 3. Effect of sulphuric acid concentration on leaching efficiency

With increasing $[\text{H}_2\text{SO}_4]$, the leaching efficiencies of Li and Fe increased, while that of P did not change significantly. At $[\text{H}_2\text{SO}_4] = 1 \text{ M}$, the leaching efficiencies of Fe, P, Li, and Al reached 3.568, 0.547, 97.53, and 12.57%, respectively. When $[\text{H}_2\text{SO}_4]$ was further increased to 1.2 M, Li leaching efficiency did not significantly change, while Fe leaching efficiency linearly increased. Thus, the optimal $[\text{H}_2\text{SO}_4]$ value was concluded to be 1 M.

3.3. Effect of the liquid-to-solid ratio on leaching efficiency

Figure 4 shows the effect of L/S on the leaching efficiencies of Fe, P, Li, and Al ($T = 90^{\circ}\text{C}$, $[\text{H}_2\text{SO}_4] = 1 \text{ M}$, $t = 1 \text{ h}$, $D = 25 \text{ g}$, $s = 150 \text{ rpm}$).

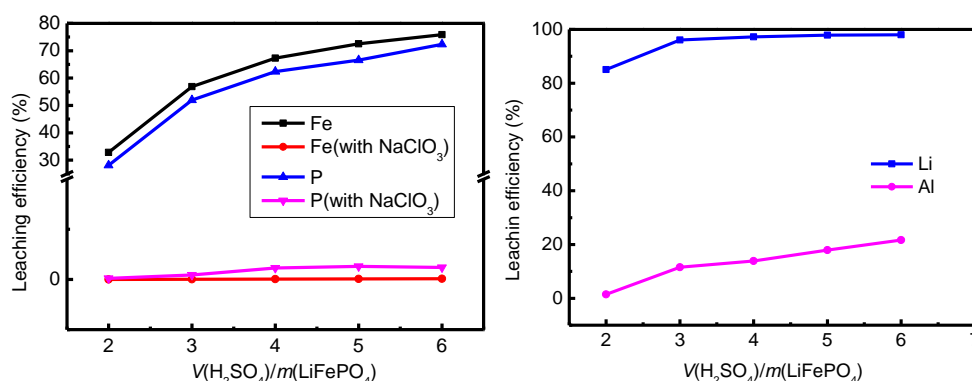


Figure 4. Effect of the liquid-to-solid ratio on leaching efficiency

An increase of L/S can reduce solution viscosity and thus accelerate mass transfer between solid and liquid phases to facilitate Li and Fe leaching. Hence, with increasing L/S, Li and Fe leaching efficiencies increased and then reached a plateau. At L/S = 5:1, the leaching efficiencies of Fe, P, Li, and Al equalled 0.26, 0.012, 97.896, and 17.93%, respectively. As these values stayed roughly constant at higher ratios, L/S = 5:1 was chosen as optimal.

3.4. Effect of leaching time on leaching efficiency

Figure 5 shows the effects of t on leaching efficiency ($T = 90^{\circ}\text{C}$, $[\text{H}_2\text{SO}_4] = 1 \text{ M}$, L/S = 5:1, $D = 25 \text{ g}$, $s = 150 \text{ rpm}$).

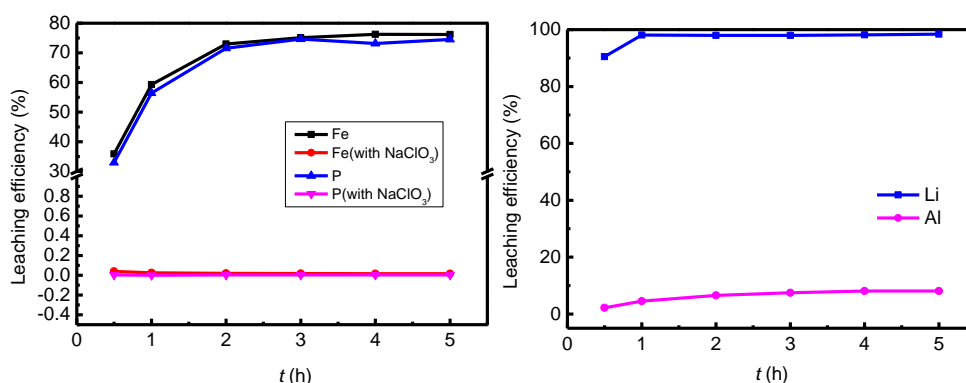


Figure 5. Effect of leaching time on leaching efficiency

With increasing t , the leaching efficiency of Li increased and then saturated, while those of Fe and P did not significantly change. After 1-h leaching, the leaching efficiencies of Fe, P, Li, and Al reached 0.025, 0.001, 98.099, and 4.54%, respectively. Thus, $t = 1 \text{ h}$ was chosen as optimal.

The leaching efficiency of P and Fe significantly increased under conventional leaching. In the presence of NaClO_3 , all Fe^{2+} ions were oxidised to Fe^{3+} and precipitated together with P as FePO_4 .

3.5. Effect of NaClO_3 dosage on leaching efficiency

Figure 6 shows the effects of D on leaching efficiency ($T = 90^{\circ}\text{C}$, $[\text{H}_2\text{SO}_4] = 1 \text{ M}$, L/S = 5:1, $t = 1 \text{ h}$, $s = 150 \text{ rpm}$).

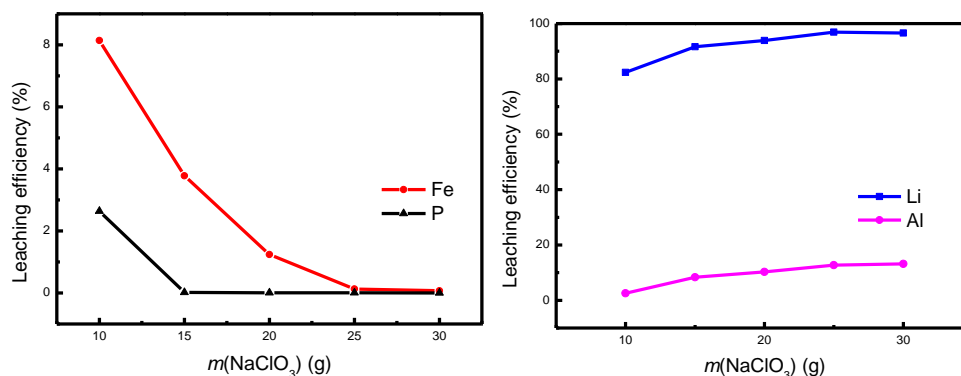


Figure 6. Effect of NaClO_3 dosage on leaching efficiency

With increasing D , the leaching efficiency of Li increased, while those of Fe and P decreased. At $D = 25$ g per 100 g raw material, Fe, P, Li, and Al leaching efficiencies reached 0.13, 0.004, 96.88, and 12.71%, respectively, and the above dosage was therefore chosen as optimal.

3.6. Effect of stirring speed on leaching efficiency

Figure 7 shows the effects of s on leaching efficiency ($T = 90^\circ\text{C}$, $[\text{H}_2\text{SO}_4] = 1\text{ M}$, $L/S = 5:1$, $t = 1\text{ h}$).

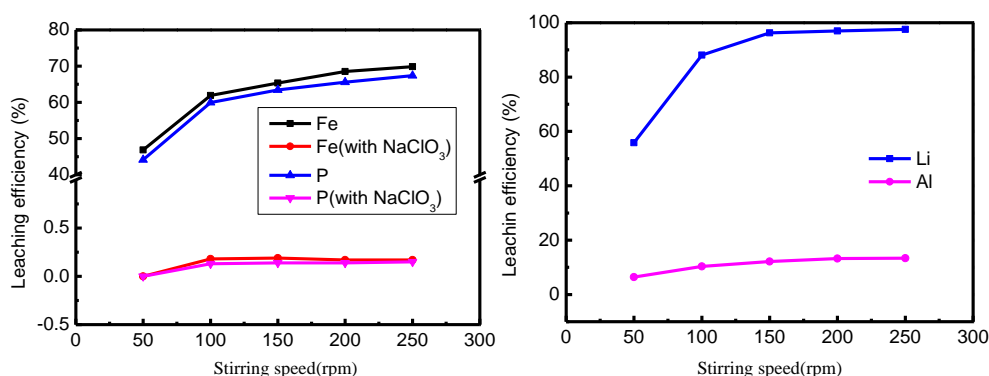
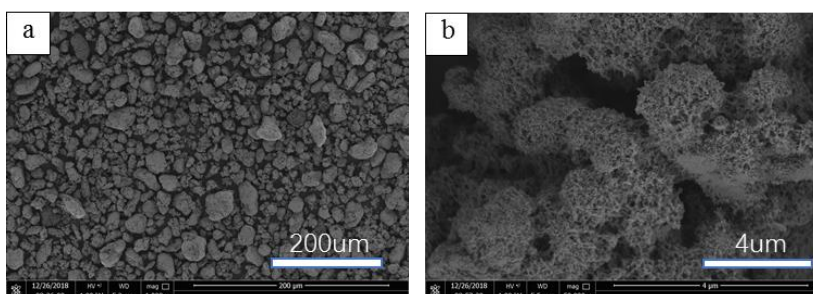


Figure 7. Effect of stirring speed on leaching efficiency

When s increased from 50 to 100 rpm, the leaching efficiencies of all elements increased. Upon a further increase to 150 rpm, P, Fe, and Al leaching efficiencies did not change significantly, while Li leaching efficiency increased to 96.26%, remaining stable at higher s . This behaviour was ascribed to the promotional effect of high stirring speed on substance diffusion.

3.7. Verification test

On the basis of single-factor experiments, optimum leaching conditions were determined as $T = 90^\circ\text{C}$, $[\text{H}_2\text{SO}_4] = 1\text{ M}$, $L/S = 5:1$, $t = 1\text{ h}$, $D = 25$ g per 100 g raw material. Under these conditions, the leaching efficiencies of Fe, P, Li, and Al equalled 0.21, 0.03, 97.23, and 11.87%, respectively.



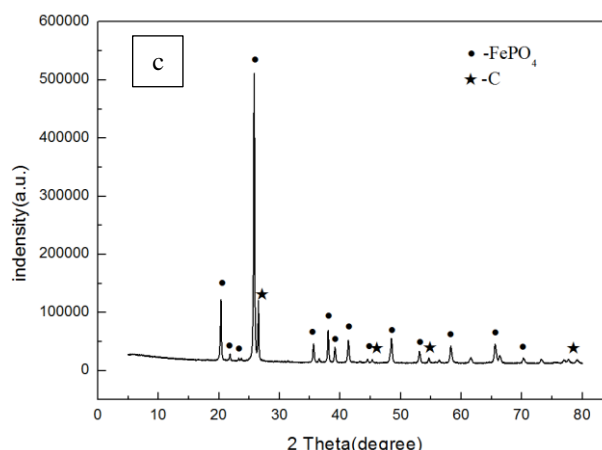


Figure 8. (a, b) SEM images and (c) XRD pattern of leaching residue

The morphological features of leaching residue particles obtained after leaching at optimum leaching conditions are displayed in Figure 8(a,b). It can be observed that the particles of leached residue are of different sizes (Figure 8a), and the surface of leached slag is of flocculent structure (Figure 8b). In order to identify the crystalline structure of leaching residue particles, XRD spectra were recorded and presented in Figure 8c. In order to identify the crystalline structure of leaching residue particles, XRD spectra were recorded and presented in Figure 8c. As can be seen from the above figures, LiFePO_4 was leached with H_2SO_4 in the presence of NaClO_3 at controlled pH and system potential, FePO_4 is the main component of the leaching residue. This indicates in the technology, we can removal of Fe in the form of insoluble FePO_4 to afford a solution of Li_2SO_4 and thus achieve selective Li leaching.

4. Conclusions

Herein, we realised selective leaching of Li from spent LiFePO_4 cathodes, showing that in the presence of NaClO_3 , all Fe^{2+} ions in solution were oxidised to Fe^{3+} and precipitated together with P as FePO_4 to afford a P- and Fe-free solution containing Li.

1) Optimum conditions for the selective leaching of LiFePO_4 were determined as leaching temperature = 90°C , $[\text{H}_2\text{SO}_4] = 1 \text{ M}$, $\text{L/S} = 5:1$, leaching time = 1 h, NaClO_3 dosage = 25 g per 100 g raw material.

2) FePO_4 can be obtained by selective leaching. After purification and modification, pure FePO_4 was obtained, which was used to prepare LiFePO_4 and realize resource recycling.

The paper, written in English, will publish on the website as .pdf file, ONE COLUMN; it should better between 4 and 12 pages. The article should be composed of the title, author(s), abstract, keywords, introduction, materials and methods, results and discussion, conclusions, and references.

References

1. ZHENG, R.J., WANG, W.H., DAI, Y.K., MA, Q.X., LIU, Y.L., MU, D.Y., LI, R.H., RENA, J., DAI, C.S., A closed-loop process for recycling $\text{LiNi}_x\text{Co}_y\text{Mn}_{(1-x-y)}\text{O}_2$ from mixed cathode materials of lithium-ion batteries, *Green Energ. Environ.*, **2**(1), 2017, 42-50.
2. BUGA M., RIZOIU A., BUBULINCA C., Study of LiFePO_4 Electrode Morphology for Li-Ion Battery Performance, *Rev. Chim.*, **69**(3), 2018, 549-552.
3. TROCOLI, R., BATTISTEL, A., MANTIA, F. L., Selectivity of a Lithium-Recovery Process Based on LiFePO_4 , *Chem-Eur. J.*, **20**(32), 2014, 9888-9891.
4. HOU, H. Y., LI, D. D., LIU, X. X., YAO, Y., DAI, Z. P., YU, C. Y., Recovery of waste Li foils from spent experimental Li-anode coin cells for LiFePO_4/C cathode, *Sustainable Mater. Techn.*, **17**, 2018,



e00064.

5. WU, Z. J., JIANG, B. F., LIU, W. M., CAO, F. B., Selective Recovery of Valuable Components from Converter Steel Slag for Preparing Multidoped FePO_4 , *Ind. Eng. Chem. Res.* **50**(24), 2011, 13778-13788.
6. YANG, Y.X., MENG, X.Q., CAO, H.B. LIN X., Selective Recovery of Lithium from Spent Lithium Iron Phosphate Batteries: A Sustainable Process, *Green Chem.*, **20**(13), 2018, 3121-3133.
7. ZHENG, Y., LIU, Y., DONG, C., WU, H.M., LIU, J.W., Research status of spent lithium iron phosphate battery recycling, *Chin. J. Power Sources*, **38**(6), 2014, 1172-1175.
8. YANG, Y.X., ZHENG, X.H., CAO, H.B., ZHAO, C.L., LIN, X., NING, P. G., ZHANG, Y., JIN, W., SUN, Z., A Closed-Loop Process for Selective Metal Recovery from Spent Lithium Iron Phosphate Batteries through Mechanochemical Activation, *ACS Sustainable Chem. Eng.*, **5**(11), 2017, 9972-9980.
9. LI, H., XING, S.Z., LIU, Y., LI, F.J., GUO, H., KUANG, G., Recovery of Lithium, Iron, and Phosphorus from Spent LiFePO_4 Batteries Using Stoichiometric Sulfuric Acid Leaching System, *ACS Sustainable Chem. Eng.*, **5**(9), 2017, 8017-8024.
10. KIM, H.S., SHIN, E.J., ChemInform Abstract: Re-synthesis and Electrochemical Characteristics of LiFePO_4 Cathode Materials Recycled from Scrap Electrodes, *Cheminform*, **34**(3), 2013, 851-855.
11. LI, L., LU, J., ZHAI, L.Y., ZHANG, X.X., CUETISS, L., JIN, Y., WU, F., CHEN, R.J., AMINE, K., A facile recovery process for cathodes from spent lithium iron phosphate batteries by using oxalic acid, *Csee J. Power Energy*, **4**(2), 2018, 219-225.
12. HE, L.H., ZHAO, Z.W., Liu, X.H., CHEN, A.L., SI, X.F., Thermodynamics analysis of LiFePO_4 precipitation from $\text{Li-Fe(II)-P-H}_2\text{O}$ system at 298 K, *T. Nonferr. Metal. Soc.*, **22**(7), 2012, 1766-1770.
13. ZHAO, Z.W., LIANG, X.X., LIU, X.H., HE, L.H., CHEN, X.Y., SI, X.F., CHEN, A.L., Thermodynamics analysis of Li-extraction from brine using FePO_4 ion-sieve, *Chin. J. Nonferrous Met.*, **23**(2), 2013, 559-567.
14. JU, H., WU, J., XU, Y.H., Revisiting the electrochemical impedance behavior of the LiFePO_4/C cathode, *J. Chem. Sci.*, **125**(3), 2013, 687-693.
15. JING, Q.K., ZHANG, J.J., LIU Y.B., YANG, C., MA, B. Z., CHEN, Y.Q., WANG, C. Y., E-pH Diagrams for the $\text{Li-Fe-P-H}_2\text{O}$ System from 298 to 473 K: Thermodynamic Analysis and Application to the Wet Chemical Processes of the LiFePO_4 Cathode Material, *J. Phys. Chem. C*, **123**(23), 2019, 14207-14215.

Manuscript received: 18.01.2020